ABLATION-RADIATION COUPLING AND VUV RADIATION ANALYSIS IN EXPANSION TUBE AND PLASMA WIND TUNNEL TESTING

Loehle S.[1], Sheikh U.[2,3], Hermann T.[1], McIntyre T.[3], Leyland P.[2], Lewis S.[3], and Wei H.[3]

[1]*High Enthalpy Flow Diagnostics Group, Institute of Space Systems (IRS), University of Stuttgart, Stuttgart, Germany*
[2]*Ecole Centrale Polytechnique de Lausanne (EPFL), Lausanne, Switzerland*
[3]*Center for Hypersonics, The University of Queensland, Brisbane, Australia*

ABSTRACT

A major contribution to the radiative heat flux for re-entering space vehicles comes from radiation in the vacuum ultraviolet (VUV) region of the electromagnetic spectrum. This, in itself, is a challenge to measure due to instantaneous absorption within facilities and flight observations unless specially designed evacuated light paths are used. Such measurements have been successfully performed at the Institute of Space Systems (IRS) in a Plasma wind tunnel (PWT) and the Centre for Hypersonics in an expansion tube on cold ab initio probes (only VUV radiation of the plasma), and on samples of carbon preforms and carbon-carbon. At IRS, tests were performed also using ASTERM, a low density ablator of Airbus Defense and Space. PWT tests were conducted in the PWK1 facility at IRS. A spectroscopic setup has been designed and qualified for measurements of VUV radiation in the boundary layer through a small bore hole in the material sample. The experimental conditions have been chosen to match a high altitude flight condition of the Hayabusa flight. Simultaneously to the VUV spectroscopy, UV/NIR spectroscopy, photogrammetric recession rate measurements and surface temperature measurements were conducted intending to investigate the radiation ablation coupling phenomena in the plasma wind tunnel testing. Expansion tube studies were conducted using the X2 facility at the Centre for Hypersonics. Three super-orbital flow conditions representative of Hayabusa and Phoebus trajectory points were used. Half-cylindrical models made of steel, cold graphite or hot pre-baked graphite each with a radius of curvature of 48 mm and width of 10 mm were tested in the facility. Spectra were obtained along the stagnation streamline in the wavelength range from 120 nm to 180 nm and calibrated for absolute radiance using a Deuterium lamp. Measurements were compared between the test models to investigate the effects of ablation on the VUV spectrum. Plasma wind tunnel experiments yielded larger molecular UV/VIS radiation for carbon preform samples as well as larger atomic VUV radiation. Pre heated samples in expansion tube experiments showed larger CN production but did not introduce new species in the VUV spectra.

Key words: High-speed Earth Re-entry, VUV Emission Spectroscopy, Expansion Tube, Plasma Wind Tunnel.

1. INTRODUCTION

Plasma wind tunnels developed at the Institute of Space Systems (IRS) of the University of Stuttgart have been developed to provide high enthalpy plasma flows for fundamental thermal protection material testing for high-speed atmospheric entry maneuvers [AKKL96]. These facilities have been layed out to simulate the thermo-chemical state in the boundary layer in front of a thermal protection material as a steady state condition. Impulse facilities developed at the Centre for Hypersonics at the University of Queensland (UQ) provide high speed flows in order to duplicate the hypersonic flow conditions in front of a re-entry vehicle [Mor97] for short experimental test times.

The only successful concept for thermal protection at these load levels are ablative heat shields. Ablative materials withstand the high heat loads through a combination of several effects: The hot surface reduces the heat transfer at the wall and increases the re-radiation of heat; pyrolysis processes inside the material lead to an outgassing which keeps the hot plasma flow (further) away from the surface; and chemical and thermal decomposition consumes heat through oxidation, nitridation, and sublimation [JGM13]. Due to the complex coupled physical phenomena of chemistry and radiation, ablation at high entry speeds is still not sufficiently understood to allow reliable predictions [HL67]. Both increase and decrease in radiative heating through ablation have been reported in numerical analysis [Gup00, Par07, JGS09]. The numerical analysis have also reported the significance of radiation in the vacuum-ultraviolet (VUV) wavelength interval, i.e. wavelengths between 80 nm and 180 nm [NPBM08, JMG+11, Par04, LWM+09, PAI98, JGM13]. Particularly when considering ablation, a coupling of radiation and flowfield is required for the understanding and accurate prediction of the surface heating processes [JGM13].

The radiation emission spectra on the stagnation line for the shock, the relaxation zone, and the boundary layer are shown in Fig. 1. These spectra are results from numerical flowfield calculations using URANUS for the peak heating re-entry condition of the Hayabusa capsule in 2010 at a velocity of $v = 10.52$ km/s and an altitude of 56.6 km (see [LBHP12] and references therein for more details). The simulation was a flowfield simulation with loose coupling to radiation. Thus, the plotted spectra are the result of the radiation transport. Ablative processes are not considered. Radiation develops at the strong shock

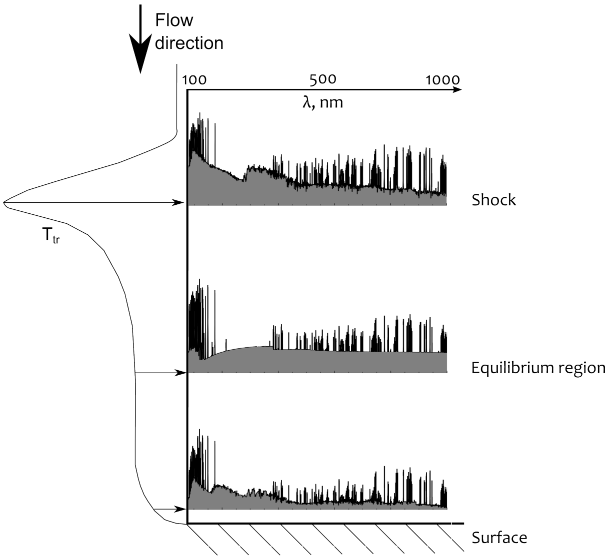

Figure 1. Principal spectral absorption and emission along the stagnation streamline. Spectra have been calculated using URANUS and PARADE for peak heating conditions of Hayabusa (reproduced from [LHZ+14]).

front and comes mostly from the VUV regime behind the shock [FWHR08]. Without ablation, the predominantely atomic VUV radiation is mainly self-absorbed in the boundary layer where a high amount of low energy and ground state particles are present. Radiative transport within the flowfield can have a significant effect on the macroscopic structure of the flow [MMB+08]. Physical phenomena involved are non-equilibrium thermal relaxation due to radiation absorption of the shock layer radiation resulting in non-equilibrium gas composition and precursor heating [JMG+11, CG13, JGM13]. Additionally, molecular radiation in the visible is present and can add a significant contribution to the radiative heat flux [Röc99]. Numerical calcuations with a coupling of radiation with the flowfield show that the convective heat flux increases and radiative heat flux decreases due to the coupling [FWHR08].

The described situation changes again when ablation products are considered. Coupled numerical calculations with ablation and radiation show that the shock distance is increased by ablation and the radiation heating is significantly reduced. Mainly C_3, atomic hydrogen (H) and carbon (C) influence the boundary layer [JGM13]. The convective heating, which is decreased by ablation, is almost unchanged due to the ablation and radiation coupling [JGS09].

The flight experiment Fire-II demonstrated the significance of VUV radiation and it has been investigated extensively in impulse facilities [Cau67, CMGO09, McC72, SMZ+12, WHAW69, Sut84]. However, to the knowledge of the authors there is only the work of Palumbo who conducted optical emission spectroscopic measurements considering the VUV wavelength interval in a plasma wind tunnel setup [PCWP97]. An experimental investigation of the coupling of ablation and radiation by means of spectroscopic tools including the VUV wavelength range was not performed to date.

This paper provides an overview of the experimental campaigns at IRS and UQ attempting to investigate experimentally the influence on ablation to the radiation issues mentioned above including tests with ablative materials. Due to the significance of the radiation below 180 nm, VUV spectroscopy has been applied in the plasma wind tunnel PWK1 to measure VUV spectra in the presence of ablative processes [HZF+14]. Furthermore, UV/NIR optical emission spectroscopy, infrared thermography, and pyrometry has been set up. A photogrammetric setup has been operated simultaneously which allows an in–situ surface analysis and recession detection [LSRC14]. Including conventional video and photography, 7 different diagnostic tools have been applied simultaneously to each test. Expansion tube experiments have been conducted measuring VUV radiation in front of a hot and cold wall graphite sample in the expansion tube X2 [She14].

The investigations are part of a research project funded by the European Space Agency (ESA) and led by the Ecole Federale Polytechnique de Lausanne (EPFL) [LMS+12].

2. PLASMA WIND TUNNEL EXPERIMENTS

Within this study material tests have been conducted in the plasma wind tunnel PWK1. Details of the facility setup for this campaign can be found in e.g. [LHZ+14]. The sample is mounted in a probe holder which is mounted on a moving platform inside the vacuum chamber. The high-enthalpy air flow is provided by a magnetoplasmadynamic arcjet generator (RD5) [AKKL96]. The probe is moved horizontally inside the chamber to adjust for heat load and total pressure. The sample material is a carbon preform of type CALCARB with a diameter of 40 mm. These preform materials are suitable for these basic ablation experiments, because of their high porosity allowing for volumetric oxidation which is assumed to occur with real lightweight ablators [HCMH12]. Calcarb is used as a simple material without a phenolic resin in order to allow the investigation of these surface effects. For comparison to the non-ablating case a cooled copper sample is mounted.

The chosen flow condition (see Tab. 1) has been investigated previously for ground test based interpretation of the Hayabusa re-entry in 2010, which was a superorbital re-entry that has been observed with instruments aboard an aircraft [LJ14, LBHP12, Jen10]. Heat flux and total pressure have been measured in a separate measurements using the same probe geometry. The local heat flux is

Table 1. Plasma wind tunnel condition corresponding to Hayabusa at 78.8 km

Parameter	Value
mass flow $\dot{m}$	$18,0\ \frac{g}{s}$
ambient pressure p_∞	$16,6$ hPa
total pressure p_{tot}	$24,3$ hPa
arc current I	1220 A
arc voltage U	133 V
electric power P	162 kW
probe position	$x = 270$ mm,$y = 0$ mm
heat flux $\dot{Q}$	$4100\ \frac{kW}{m^2}$
mass–specific enthalpy h	$68,43\ \frac{MJ}{kg}$

measured as a cold wall heat flux on copper. The copper has been preoxidized. This surface state is considered as the one with the highest catalycity [LAK00]. The flow condition has been adjusted according to the similarity parameters derived by Kolesnikov [Kol99]. By duplicating total pressure, local mass–specific enthalpy and the boundary layer velocity gradient in a subsonic plasma flow, the boundary layer of a flight condition with respect to convective heat transfer is reproduced. The local mass–specific enthalpy has been determined from the measured cold wall heat flux and the semi-empirical formula of Zoby [Zob68]. Velocity measurements to investigate the boundary layer velocity gradient have not been performed at this condition so far. The duplication of the radiation has not been considered by Kolesnikov.

There are only few optical accesses available at the vacuum chamber. Fig. 2 shows a top view schematic of the arrangement of the mentioned experimental systems. The

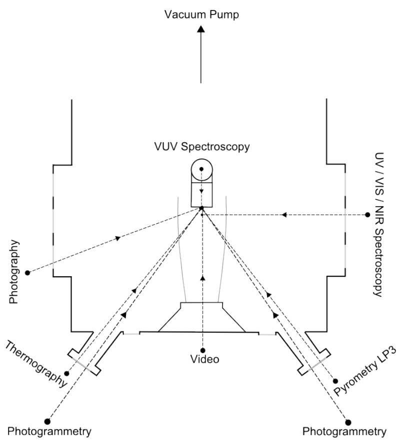

Figure 2. Schematic of the arrangement of the suite of 7 different diagnostic setups at the wind tunnel (top view).

vacuum-ultraviolet spectroscopy is designed to measure through the sample as it has been performed by Palumbo et al. [PCWP97]. The measured radiation is directed with mirrors outside the vessel to the spectrometer mounted on top of the vacuum chamber. The UV/VIS spectroscopy is arranged on the side of the vacuum chamber. The boundary layer has been investigated using the classical optical emission spectroscopic setup as it has been applied by several researchers at IRS [RAK97]. Thermography and Pyrometry are applied through two windows in the front lid. The same windows have been used for the photogrammetric setup [LSRC14]. Through additional windows, videos and photos are taken.

Both samples (copper or Calcarb) have the same front geometry, i.e. a 40 mm diameter. The samples are mounted in a water cooled housing. The copper sample is separately water cooled in order to determine the surface heat flux onto the circular 40 mm diameter front surface area.

Testing is conducted as follows: The sample is positioned laterally outside the flow. Usually, the required test condition is reached after about 3-5 min. When all parameters are steady, the sample is laterally moved into the flow to the center axis. The test time starts ($t = 0$ s) when the position is reached. After the specified test time (typically 30 - 45 s, the generator power is cut and the gas mass flow valves are closed quickly. The sample lasts at its position. The power off command is defined as the test end.

2.1. Optical Emission Spectroscopy

The measurements of the radiation are undertaken using optical emission spectroscopy. In this work two spectrometers have been implemented, a VUV spectrometer measuring the 116–197 nm wavelength region and a UV-NIR spectrometer covering the 300–960 nm range.

The VUV measurements are captured utilising an ACTON RESEARCH CORPORATION VM-521-SG 1 m focal length spectrometer coupled with an ANDOR iStar 340T intensified charge-coupled device (CCD) camera. The spectrometer has been provided by EPFL and the camera and calibration lamp were provided by the Centre for Hypersonics (UQ) (of the University of Queensland). An evacuated light path for the VUV spectroscopy has been designed to redirect the emitted radiation from the stagnation point of the probe to the entrance of the spectrometer. The line of sight has been tilted by 28° in order to avoid a direct view towards the generator (see Fig. 8). A MgF_2 window is located at the rear end of the sample which seals the light path, directly behind this is a mirror to redirect the radiation to the rear of the probe and then out of the test section where it is focussed onto the spectrometer entrance slit. This configuration is shown in Fig. 8. The evacuated light path is maintained at a vacuum lower than 5×10^{-5} hPa which has been shown to prevent significant absorption.

Calibration of the VUV system is conducted using a MCPHERSON 632 deuterium lamp. The lamp has been calibrated by the Physikalisch-Technische Bundesanstalt Berlin (Germany's national metrology institute). Pre- and post-test the lamp is mounted in front of the test setup and recordings are taken to measure the spectral response of

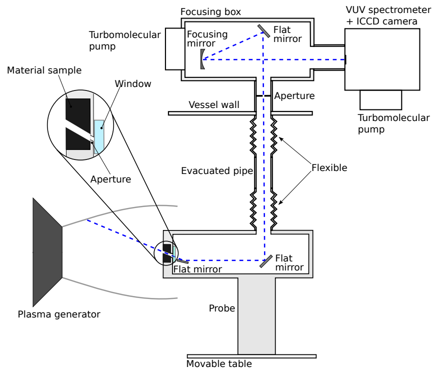

Figure 3. Schematic of the VUV setup (side view).

the VUV system. The material sample needs to be removed to be able to evacuate the optical path between the MgF_2 window and the calibration lamp. This does not affect the required comparability of the calibration configuration with the plasma wind tunnel configuration as long as the window with possible contamination is kept untouched. Full details of the setup, initial testing, calibration and preliminary results can be found in Ref. [HZF+14] .

The UV-NIR measurements are taken with a PRINCETON INSTRUMENTS SpectraPro 2758 spectrometer coupled with an ANDOR DU920N-0E camera. This optical system images a vertically orientated rectangular region 60 mm high and 1.6 mm wide at approximately 5 mm in front of the probe (for further details see [LHZ+14]). Measurements are taken with a 300 l/mm grating over a range of different central wavelengths covering the full wavelength region from 300–960 nm. The separately acquired spectra covering 120 nm each are concatenated during post-processing to give the full spectrum. The UV-NIR system is calibrated using a GIGAHERTZ-OPTIK BN0102 integrating sphere for absolute radiance (intensity). This is done by positioning the integrating sphere at the measurement position and taking calibration measurements over the full spectral range.

The ablation situation has been further investigated using additional diagnostics mounted in parallel. Surface temperature has been measured using an LP3 linear pyrometer from KE TECHNOLOGIE GMBH at 950 nm. A recently procured thermographic camera system of LUMASENSE Mikron MCS640 is a commercial camera layed out and calibrated by the manufacturer for the optical paths at IRS. It measures with a frame rate of 60 fps. The measured data is also corrected for window transmission and surface emissivity. The recession of the ablating samples has been analysed using stereoscopic photogrammetry. Stereoscopic photogrammetry allows for 3D surface imaging during wind tunnel testing using two digital single lens reflex (DSLR) cameras. With the photogrammetric analysis as developed at IRS, the surface is resolved with 25000 px/cm^2, approximately 400 dpi. This allows the in-situ analysis of the recession phenomena of the ablator [LSRC14].

3. EXPANSION TUBE EXPERIMENTS

This section outlines the experiments in the X2 expansion tube. The test matrix can be broken down into two experimental campaigns: experiments measuring VUV radiation incident and across the surface of a rectangular steel model, and experiments to observe changes in VUV emission due to an ablating graphite surface. Three conditions representative of Hayabusa and Phoebus re-entry trajectory points were utilised for both campaigns and are outlined in Table 2.

Table 2. Static freestream testing conditions for X2 experiments.

Condition	Med.-C	Med.-B	Fast-A
Velocity (km/s)	9.30	10.2	10.6
Temperature (K)	2570	2700	3120
Pressure (Pa)	1690	866	2840
Density (kg/m^3)	0.00223	0.00104	0.00280
Enthalpy (MJ/kg)	46.7	57.7	62.2
Total Pressure (GPa)	5.00	4.67	xx

The emission spectroscopy system utilised in these experiments consisted of a McPherson NOVA 225 spectrometer coupled to an Andor iStar generation 2 ICCD capable of measuring down to 115 nm. The system was calibrated using the same McPherson deuterium lamp as outlined in Section 2.1. An adaptor plate was utilised to position the lamp at the location of the radiating shock layer, allowing for an in-situ calibration. A high vacuum optical chamber was coupled to the spectrometer and test section to remove oxygen and water vapour from the optical path. Depending on the viewing configuration, the optical path was sealed at the surface of the model, or the across surface viewing port, again with a MgF_2 window. The across surface viewing port was housed within a fence that created an acute shock wave dissociating the gas directly in front of the window. A 10 mm gap was maintained between the model and the fence, ensuring negligible absorption of VUV radiation between the radiating shock layer and the high vacuum optical path, and enough distance to avoid any disturbance to the shock layer being observed. An annotated image of this configuration is shown in Fig. 4 and a full outline of this system can be found in [She14].

3.1. Incident and Across Surface Measurements

A simple two-dimension geometry was selected for this series of experiments to reduce modelling complexity, allow for windows to be embedded in the surface of the model without disturbing the surface shape, and provide a large shock stand off. The model shape selected was a rectangular bar normal to the flow with a length of 90 mm and a height of 25 mm. These dimensions were selected to provide the highest aspect ratio model that could be contained within the core flow of the X2 expansion tube

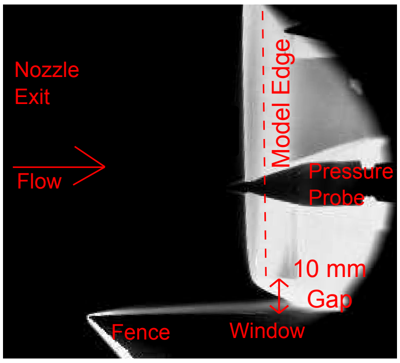

Figure 4. Annotated top down image acquired during the test time illustrating the shock wave created by the fence not interacting with the shock layer around the model. The observational window position is centred upstream of the surface of the model at a distance of 10 mm [SMM14].

and house an appropriately thick stock size magnesium fluoride window.

Two sets of measurements at all three conditions were made using this system. The first set of measurements was spatially resolved emission measurements across the surface of the model, viewing through an optical port as shown in Fig. 4. Incident spectral measurements through the surface of the model were also carried out using a turning mirror within the test section and coupling to the external focussing optical system. The optical systems utilised for both sets of measurements is shown in Fig. 5.

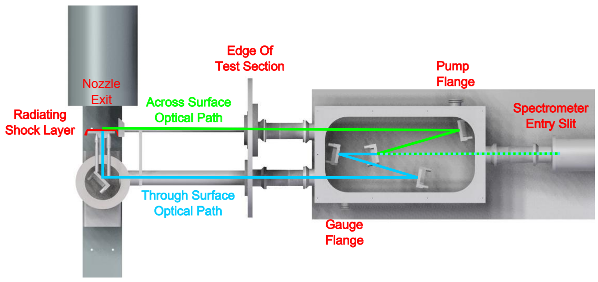

Figure 5. Imaging optics to observe radiation across and through the surface of the models. Image drawn to scale [SMM14].

3.2. Ablating Model Experiments

This series of experiments was conducted using half-cylindrical models with an outer diameter of 49 mm and a width of 10 mm. The goal of these experiments was to investigate changes in radiative emission in the VUV with an ablating graphite surface compared with a steel surface. Carbon is found in the expansion tube freestream in trace amounts and therefore an emission baseline was established using steel models. Cold and pre-heated graphite models were tested to investigate possible changes in VUV emission. Pre-heated graphite tests were conducted using the resistive pre-heating technique developed by Zander [ZMS+12]. The graphite selected for these tests was Graphtek GM-10 due to its isotropic properties allowing for a uniform surface temperature distribution [Gra14]. The temperatures achieved by pre-heated graphite samples were in excess of 2000 K and two colour ratio pyrometery was utilised to obtain two-dimensional temperature maps of the samples using images taken seconds before the experiment.

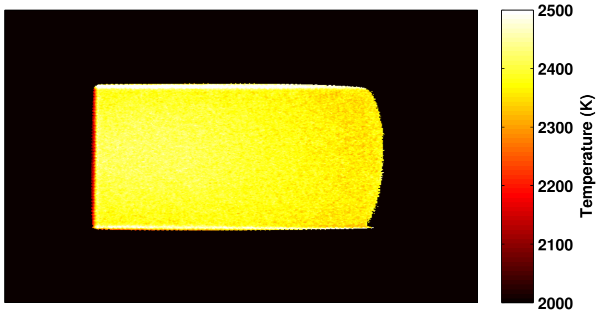

Figure 6. Temperature map of a pre-heated graphite model. Flow from left to right in image [SIW+14].

Pre-heating of samples resulted in additional complexities to the experimental setup. The viewing window at the end of the optical path is required to be 10 mm from the radiating shock layer and therefore experiences a significant heat flux during the pre-heating process. Furthermore, it was found that out-gassing of volatiles in the pre-heating process coated the window and significantly reduced transmission before the commencement of test time. A study was conducted by Wolter to modify the existing configuration to enable VUV spectral measurements of pre-heated graphite models [Wol14]. It was concluded that models required up to ten pre-heating cycles under vacuum to remove all volatiles. Additionally, the surface of the fence was recessed and a copper piece installed to remove the radiative heat flux onto the glue behind the window. Combining these modifications, and completing the experiment within seconds of the model achieving steady state temperature, ensured no damage occurred to the windows before the conclusion of the test time. The final model configuration is shown in Fig. 7.

4. RESULTS AND DISCUSSION

In the following the results from the two facilities are summarised in separate subsections. Then a first conclusion from the results from both test campaigns is tried sehe ich bisher noch nicht.

4.1. Plasma Wind Tunnel Experiments

Figure 8 shows the measured VUV radiance (spectral and cumulative) of a cooled copper and Calcarb material sample which features strong atomic lines of oxy-

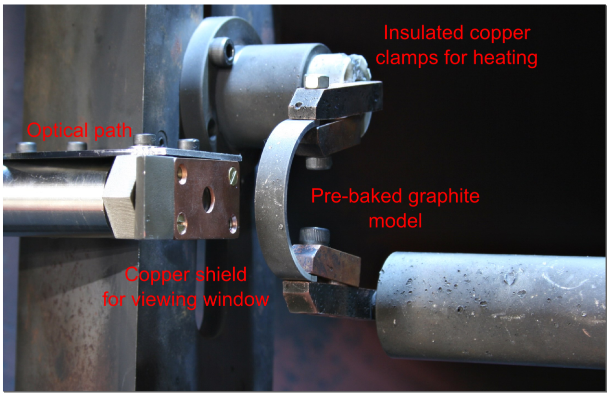

Figure 7. Configuration of graphite model with insulated heating clamps and shielded optical port [SIW+14].

gen and nitrogen for both cases. Atomic carbon lines are also present in the Calcarb spectrum. The spectral region between 148 and 169 nm of the Calcarb spectrum could not be calibrated correctly and was partially oversaturated and is therefore neglected for the cumulative radiance. The Calcarb spectrum exhibits stronger radiation of nitrogen lines than the copper case, however, the oxygen triplet at 130 nm is almost identical in the two cases. Figure 9 shows the UV-VIS local emission coefficient (spectral and cumulative) of the stagnation streamline 5 mm in front of a cooled copper and Calcarb material sample. The atomic radiation of both nitrogen and oxygen is stronger in the case of Calcarb. Furthermore, the molecular radiation of N_2 and N_2^+ is also stronger for Calcarb which also exhibits additional radiation of the CN violet band.

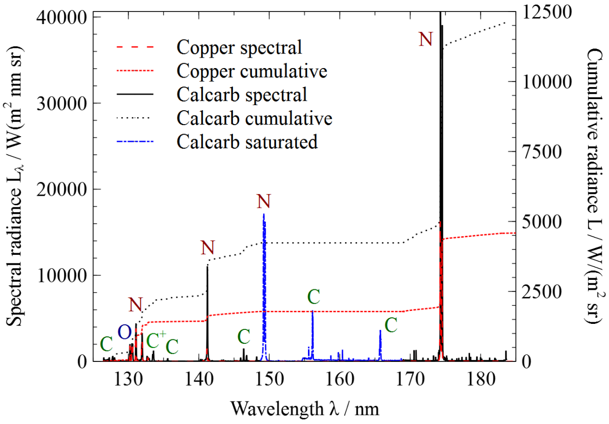

Figure 8. VUV spectrum in front of the sample.

Both spectral regions show that atomic and molecular radiation is stronger for the Calcarb sample. A possible explanation could be a higher surface temperature leading to a higher gas temperature in the boundary layer. In front of the copper sample, the emission spectra have been analysed assuming a Boltzmann distribution for ro-

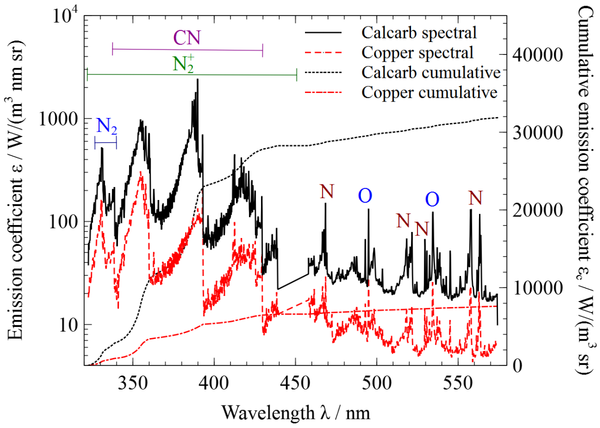

Figure 9. UV-NIR stagnation streamline spectrum 5 mm in front of the sample surface.

tational and vibrational states. This results in a rotational temperature of $T_{\mathrm{rot}} = 13270\,K$, a vibrational temperature of $T_{\mathrm{vib}} = 12750\,K$ and an electronic excitation temperature $T_{\mathrm{exc}} = 8300\,K$. The measurements in the visible and NIR have been complemented by the VUV data on atomic oxygen, i.e. the ground and low lying energy states have been taken into account. The details of this approach are currently in preparation for further publication. The respective data analysis for the hot Calcarb sample is still in progress.

4.2. Expansion Tube Experiments

A substantial experimental dataset has been acquired through the course of the ARC grant. Rectangular models with two optical configurations, and three half-cylindrical models with one optical configuration, have been tested for all three conditions presented in Table 2. The rectangular model experiments provide spatial resolution when viewed from across the surface and spectrally resolved measurements of VUV radiation incident on the surface at the stagnation point, and experimental results were previously presented at EUCASS [LMM+13]. Initial analysis of the heated and cold half-cylinder models shows no new species in the VUV spectral range due to an ablating surface, as shown in Fig. 10. There was significantly increased cyanogen production observed for the heated models indicating ablation of the heated models [SIW+14]. Further investigation of the carbon lines measured is required before conclusions in regards to VUV emission for heated models with an ablating surface can be drawn.

5. SUMMARY

Experiments aiming to investigate ablation-radiation coupling have been sucessfully conducted in the plasma wind

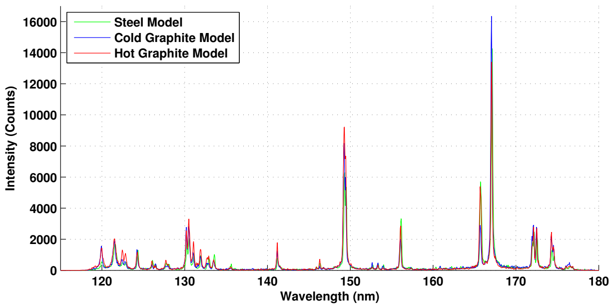

Figure 10. Comparison of shock layer spectra using steel, cold graphite and pre-heated graphite models for the Medium-B condition.

tunnel PWK1 as well as in the expansion tube X2. Optical emission spectroscopic measurement systems in different wavelength intervals have been applied to investigate the radiation of the hot flow in front of cold metallic reference materials as well as carbon samples. The planned experiments have all been conducted and a comprehensive set of data for both plasma wind tunnel and expansion tube is available for further ablation-radiation coupling assessment.

Spectra obtained through experiments in the expansion tube with cold steel, cold graphite and hot graphite samples do not exhibit a clear trend. Further investigation of the measurement results is required.

Plasma wind tunnel experiments show stronger radiation from both molecules and atoms for the hot Calcarb samples in comparison with cooled copper. The influence of ablation on the measured radiation is significant. Through the combination of flowfield spectroscopy upstream the sample, a detailed investigation of the radiation transport effects becomes accessible.

The combination of the two experimental campaigns will then allow a better understanding of the ablation radiation coupling.

6. ACKNOWLEDGEMENT

The authors gratefully acknowledge the financial support by the European Space Agency ESA through the research grant No.2011/ITT-6632/PL.

REFERENCES

[AKKL96] M. Auweter-Kurtz, H. Kurtz, and S. Laure. Plasma generators for re-entry simulation. *Journal of Propulsion and Power*, 12(6):1053–1061, November-Dezember 1996.

[Cau67] D. L. Cauchon. Radiative heating results from the fire-ii flight experiment at a reentry velocity of 11.4 kilometer per second. Technical Report TM X-1402, NASA, July 1967.

[CG13] Y.-K. Chen and T. Gökçen. Effect of nonequilibrium surface thermochemistry in simulation of carbon-based ablators. *AIAA Journal of Spacecrafts and Rockets*, 50(3), 2013.

[CMGO09] B. Cruden, R. Martinez, J. H. Grinstead, and J. Olejniczak. Simultaneous vacuum ultraviolet through near ir absolute radiation measurement with spatiotemporal resolution in an electric arc shock tube. In *41st Thermophysics Conference*. AIAA, 2009.

[FWHR08] M. Fertig, M. Winter, G. Herdrich, and H.-P. Röser. Modelling of high speed earth entry, study note p 2.2. Interner Bericht IRS-08-P1, Institut für Raumfahrtsysteme, Universität Stuttgart, 2008.

[Gra14] http://www.graphtekllc.com/grades.htm Graphtek. Graphtek materials table, Nov 2014.

[Gup00] R. N. Gupta. Aerothermodynamic analysis of stardust sample return capsule with coupled radiation and ablation. *Journal of Spacecraft and Rockets*, 37(4):507–514, July 2000.

[HCMH12] B. Helber, O. Chazot, T. Magin, and A. Hubin. Ablation of carbon preform in the vki plasmatron. In *43d Thermophysics Conference*, number AIAA 2012-2876. AIAA, 2012.

[HL67] H. Hoshizaki and L. E. Lasher. Convective and radiative heat transfer to an ablating body. In *Thermophysics Conference*, number AIAA-67-327. AIAA, 1967.

[HZF+14] T. Hermann, F. Zander, H. Fulge, S. Löhle, and S. Fasoulas. Experimental setup for vacuum ultraviolet spectroscopy for earth re-entry testing. In *30th Aerodynamic Measurement Technology and Ground Testing Conference*. AIAA, 2014.

[Jen10] P. Jenniskens. Hayabusa capsule entry airborne observation campaign, 2010.

[JGM13] C. O. Johnston, P. A. Gnoffo, and A. Mazaheri. Influence of coupled radiation and ablation on the aerothermodynamic environment of planetary entry vehicles. In *Radiation and Gas-Surface Interaction Phenomena*, volume 218 of *RTO Lecture Series*, 2013.

[JGS09] C. O. Johnston, P. A. Gnoffo, and K. Sutton. Influence of ablation on radiative heating for earth entry. *Journal of Spacecrafts and Rockets*, 46:481–491, 2009.

[JMG+11] C. O. Johnston, A. Mazaheri, P. A. Gnoffo, B. Kleb, K. Sutton, D. Prabhu, A. M. Brandis, and D. Bose. Assessment of radiative heating uncertainty for hyperbolic earth entry. In *42nd AIAA Thermophysics Conference*, June 2011.

[Kol99] A. F. Kolesnikov. Extrapolation from high enthalpy tests to flight based on the concept of local heat transfer simulatino. In *Measurement Techniques for High Enthalpy and Plasma Flows*, number 8B, Rhode–Saint–Genese, Belgium, 1999. VKI, RTO — Research and Technology Organization.

[LAK00] T. Laux and M. Auweter-Kurtz. Untersuchung des passiv–aktiv–übergangs an ssic in sauerstoffplasmen. In *DGLR–Jahrestagung*, Leipzig, 2000. DGLR–JT2000-207.

[LBHP12] S. Löhle, A. Brandis, T. Hermann, and J. Peter. Numerical investigation of the re-entry flight of hayabusa and comparison to flight and ground testing data. In *43rd AIAA Thermophysics Conference*, LA, 2012. AIAA.

[LHZ+14] S. Löhle, T. Hermann, F. Zander, H. Fulge, and T. Marynowski. Ablation radiation coupling investigation in earth re-entry using plasma wind tunnel experiments. In *30th Aerodynamic Measurement Technology and Ground Testing Conference*. AIAA, 2014.

[LJ14] S. Loehle and P. Jenniskens. High resolution spectroscopy of the hayabusa re-entry using a fabry-perot interferometer. *Journal of Spacecrafts and Rockets*, 2014. in press.

[LMM+13] P Leyland, T McIntyre, R Morgan, P Jacobs, F Zander, U Sheikh, T Eichmann, E Fahy, O Joshi, G Duffa, et al. Radiation-ablation coupling for capsule reentry heating via simulation and expansion tube investigations. In *5th European Conference for Aeronautics and Space Sciences (EUCASS)*, 2013.

[LMS+12] P. Leyland, T. McIntyre, U. Sheikh, T. Eichman, F. Zander, R. Morgan, S. Löhle, T. Hermann, F. De Filipis, E. Trifoni, and G. Cillo. Vuv radiation measurements for ablation-radiation coupling. In *ESA Radiation of High Temperature Gases Workshop*. ESA, 2012.

[LSRC14] S. Löhle, T. Staebler, T. Reimer, and A. Cefalu. Photogrammetric surface analysis of ablation processes in high enthalpy air plasma flow. In *30th Aerodynamic Measurement Technology and Ground Testing Conference*. AIAA, 2014. submitted.

[LWM+09] C. O. Laux, M. Winter, J. A. Merrifield, Arthur Smith, and P. Tran. Influence of ablation products on the radiation at the surface of a blunt hypersonic vehicle at 10 km/s. In *41st AIAA Thermophysics Conference*, number AIAA 2009-3925, 2009.

[McC72] J. O. McClenahan. Vacuum ultraviolet line radiation measurements of a shock-heated nitrogen plasma. Technical Report NASA TN D-6920, Ames Research Center, Moffet Field, California, August 1972.

[MMB+08] R. Morgan, T. McIntyre, D. Buttsworth, P. Jacobs, D. Potter, A. M. Brandis, R. Gollan, C. Jacobs, B. Capra, M. McGilvray, and T. Eichman. Impulse facilities for the simulation of hypersonic radiating flows. In *38th Fluid Dynamics Conference and Exhibit*, June 2008.

[Mor97] R. Morgan. Superorbital expansion tubes. In *21st International Symposium on Shock Waves*, July 1997.

[NPBM08] Jae Na, Chul Park, Seung-Wook Baek, and Jean Muylaert. *Preliminary Design of Super-Orbital Earth Entry Flight Experiment Using VOLNA Launcher*. Aerospace Sciences Meetings. American Institute of Aeronautics and Astronautics, may 2008. doi:10.2514/6.2008-1129.

[PAI98] Chul Park, Takashi Abe, and Yoshifumi Inatani. Research on the heatshield for muses-c earth reentry. In *7th AIAA/ASME Joint Thermophysics and Heat Transfer Conference*. AIAA, 1998.

[Par04] C. Park. Stagnation-point radiation for apollo 4. *Journal of Thermophysics and Heat Transfer*, 18(3):349–357, July 2004.

[Par07] C. Park. Calculation of stagnation-point heating rates associated with stardust vehicle. *AIAA Journal of Spacecrafts and Rockets*, 44(1), 2007.

[PCWP97] G. Palumbo, R. A. Craig, E. Whiting, and C. Park. Measured specific intensity from 130 to 900nm at the stagnation point of a model in an arcjet flow of 7.8km/s. *Journal of Quantitative Spectroscopy and Radiative Transfer*, 57(2):207–236, 1997.

[RAK97] W. Röck and M. Auweter-Kurtz. Spectral measurements in the boundary layer of probes in nitrogen/methane plasma flows. In *32nd Thermophysics Conference*, Atlanta, GA, June 23-25 1997. AIAA-1997-2525.

[Röc99] W. Röck. *Simulation des Eintritts einer Sonde in die Atmosphäre des Saturnmondes Titan in einem Plasmawindkanal*. PhD thesis, Institut für Raumfahrtsysteme, Universität Stuttgart, Germany, 1999. (in German).

[She14] U. Sheikh. *Re-Entry Radiation Aerothermodynamics in the Vacuum Ultraviolet*. PhD thesis, University of Queensland, 2014.

[SIW+14] U. A. Sheikh, M. Ibrahim, H. Wei, R.G. Morgan, and T.J. McIntyre. Filtered two-dimensional imaging in the x2 expansion tube. In *6th International Workshop on Radiation of High Temperature Gases in Atmospheric Entry*, submitted 2014.

[SMM14] U. A Sheikh, R. G Morgan, and T.J McIntyre. Vacuum ultraviolet spectral measurements for superorbital earth entry in the x2 expansion tube. *AIAA (Submitted)*, 2014.

[SMZ+12] U. Sheikh, R. Morgan, F. Zander, T. Eichman, and T. McIntyre. Vacuum ultraviolet emission spectroscopy system for superorbital reentries. In *18th AIAA/3AF International Space Planes and Hypersonic Systems and Technologies Conference*. AIAA, 2012.

[Sut84] K. Sutton. Air radiation revisited. In *AIAA 19th Thermophysics Conference*, June 1984.

[WHAW69] A. D. Wood, H. Hoshizaki, J. C. Andrews, and K. H. Wilson. Measurements of the total radiant intensity of air. *AIAA Journal*, 7(1):130–139, January 1969.

[Wol14] M.E. Wolter. Cooling of the optical access to x2. Master's thesis, Universitat der Bundeswehr Munchen, 2014.

[ZMS+12] F. Zander, R. G. Morgan, U. A. Sheikh, D. G. Buttsworth, and P. R. Teakle. Hot wall reentry testing in hypersonic impulse facilities. *AIAA*, 51:476–484, 2012.

[Zob68] E. V. Zoby. Empirical stagnation-point heat-transfer relation in several gas mixtures at high enthalpy levels. *NASA Technical Note*, (TN D-4799), 1968.